Astronomy & Astrophysics manuscript no. CoRoT*2009*symposium
February 17, 2009

Searching For Transiting Circumbinary Planets in CoRoT ⋆ and Ground-Based Data Using CB-BLS

A. Ofir[1], H. J. Deeg[2], and C. H. S. Lacy[3]

[1] School of Physics and Astronomy, Raymond and Beverly Sackler Faculty of Exact Sciences, Tel Aviv University, Tel Aviv, Israel. e-mail: avivofir@wise.tau.ac.il
[2] Instituto de Astrofisica de Canarias, C. Via Lactea S/N, 38205 La Laguna, Tenerife, Spain
[3] Department of Physics, University of Arkansas, Fayetteville, AR 72701, USA

Received XXX; accepted YYY

ABSTRACT

Aims. Already from the initial discoveries of extrasolar planets it was apparent that their population and environments are far more diverse than initially postulated. Discovering circumbinary (CB) planets will have many implications, and in this context it will again substantially diversify the environments that produce and sustain planets. We search for transiting CB planets around eclipsing binaries (EBs).
Methods. CB-BLS is a recently-introduced algorithm for the detection of transiting CB planets around EBs. We describe progress in search sensitivity, generality and capability of CB-BLS, and detection tests of CB-BLS on simulated data. We also describe a method for the correct detrending of intrinsically-variable stars.
Results. We present some blind-tests with simulated planets injected to real CoRoT data. The presented upgrades to CB-BLS allowed it to detect all the blind tests successfully. We also process real data from observations by the TrES planet search, and present some of the first results of applying CB-BLS to multiple real light curves from a wide-field survey.
Conclusions. CB-BLS is now mature enough for its application to real data, and the presented processing scheme will serve as the template for our future applications of CB-BLS to data from wide-field surveys such as CoRoT. Still, searching for transiting CB planets is still a learning experience, similarly to the state of transiting planets around single stars only a few years ago. The recent rapid progress in this front, coupled with the exquisite quality of space-based photometry, allows to realistically expect that if transiting CB planets exist - then they will soon be found.

Key words. methods: data analysis – stars: variables: general – stars: planetary systems – occultations – binaries: eclipsing

1. Introduction

Bound binary stars are one of the most common environments in the Galaxy. Studying planet formation and evolution without accounting for binary (and multiple) star systems is surely incomplete – so we aim to try to fill-in observational data on these types of systems. To help achieve this goal a Binaries Working Group was recently formed within CoRoT Exoplanets Science Team of the CoRoT space mission (Baglin *et al.* 2006) to coordinate the different searches for planets in binary systems, and we report on one of the activities within the Working Group, namely - transit searches using the CB-BLS algorithm (Ofir 2008, hereafter paper I).

Stable planetary orbits in stellar binary systems have been traditionally separated into two main families [Dvorak 1986]: in wide binaries a planet can orbit closer to- and around- one of the binary components (S-type orbit). In tight binaries stable orbits exist outside and around both components (P-type orbit - hereafter also circumbinary, or CB, planets). Holman and Wiegert (1999) had investigated the long-term stability of both S-type and P-type orbits and had shown that planetary orbits in binary systems can remain stable for a surprisingly wide range orbits.

There are many detection techniques for planets in binaries: Some are common to planets around single stars (such as: radial velocity (RV), transits, astrometry and microlensing [Muterspaugh *et al.* 2007, Lee *et al.* 2008]) and some are unique to binaries (such as: eclipse timing, gravitational waves [Seto 2008]). Generally speaking, in each geometry (i.e., S- and P- type orbits) techniques that are in principal the same take on different emphasizes.

In this paper we will focus on transits of CB planets, and specifically transiting CB planets around eclipsing binaries (EBs). In the following we list the accumulated additions to CB-BLS since paper I in §2, describe blind tests to CB-BLS in §3, and show examples from the first application of CB-BLS to real data in §4, and conclude.

2. Accumulated Additions to CB-BLS

The following describe additions to the CB-BLS implementation starting from the version used to generate the results of paper I (internally designated as version 0.51) till now (version 0.83). While the basic idea of orbit fitting remains unchanged, the specific implementation had improved sig-

⋆ Based on observations obtained with CoRoT, a space project operated by the French Space Agency, CNES, with participation of the Science Programme of ESA, ESTEC/RSSD, Austria, Belgium, Brazil, Germany and Spain.

nificantly in search sensitivity, generality, speed and results analysis. To avoid extensive repetitions, we assume in the following that the reader is familiar with paper I. We note that we plan to release the CB-BLS source code (written in `MATLAB`) in the future. CB-BLS now:

- Allow to include the surface brightness ratio (J) in the input, which increases sensitivity. See more in §2.1.
- Allow to naturally use the more accurate Roche-lobe geometry. All the user has to do is to specify the surface potentials $\Omega_{1,2}$ – which are the direct outputs of EB modeling – instead of the radii. CB-BLS then computes the 3D shape of the surface, rotates the shape to the binary inclination, and computes the silhouette of the sky-projected shape at each binary phase. CB-BLS allows single-surface binaries (contact binaries) too – which are common. We note that using this feature slows CB-BLS significantly. We comment that this feature was forecasted in paper 1 (§3.2) and is implemented along these lines.
- Account for EB inclination. The EB orbital inclination is calculated anyhow during the EB modeling, so the 2D (instead of 1D, as in paper I) sky-projected orbit for each component is computed - and the 2D distance from the test planetary model found. The planetary orbit is still assumed edge-on, but this is a good approximation since the planet is farther away from the baricenter than the EB components, and so it's alignment requirements are more stringent to begin with.
- Enable the simultaneous solution of multiple light curves of the same system, each with it's own EB model - which also allows to use multi-band data in a single run. Since after regularization (see paper I §3.3) the transit signal should be achromatic - the CB-BLS statistic can be calculated using all the regularized residuals – regardless of band. We note that multi-band solution and using the (single) surface brightness ratio J are mutually exclusive.
- Include the directional correction (Tingley 2003) - ignores negative depths.
- Allow to output all the computed CB-BLS values (and not just the maximal one for each orbital period) to allow to properly account for the sample of fitted models [Ofir 2009].
- Better visualize results for analysis, have improved robustness, better speed optimization, more input control, bug fixes etc.
- Includes a set of utilities: CB transit predictor, nonlinear optimization.

We stress that CB-BLS is a *detection* algorithm, and as such - concisely avoids many complicating elements that are known to affect the shape of the transit light curve, including: stellar limb darkening, motion of EB components along the line of sight (the very basis of RV and eclipse timing techniques), EB apsidal motion or period change, planetary eccentricity and obliquity, non-Keplerian (especially Newtonian) motions, etc. The reason none of these is included is discussed in the last paragraph of the following section.

2.1. CB-BLS with a single depth

If the EB surface brightness ratio is J is known (and J is a natural output of most, if not all, EB modeling tools) then the depth ratio between transits in front of the primary and the secondary EB components will also be J, and eq. 1 in paper I can then be re-written with just a single fitted depth as (note the last term):

$$D = \sum_k w_k (x_k - H)^2 + \sum_i w_i (x_i - L)^2 + \sum_j w_j (x_j - JL)^2 \quad (1)$$

Here we approximate L_2 from paper I to JL, which is an approximation to the correct value of $J(L+H)$. The approximation is good as long as $|H| \ll |L|$, which is the case for low duty-cycle signals such as transits. As in BLS (Kovács *et al.* 2002) and CB-BLS paper I, minimization allows to analytically compute H (unchanged) and L (revised):

$$H = \frac{-(s_1 + s_1)}{1 - (r_1 + r_2)} \quad , \quad L = \frac{s_1 + J s_2}{r_1 + J^2 r_2} \quad (2)$$

Where the $r_{1,2}$ and $s_{1,2}$ are simple sums of the data and the weights as in paper I. Plugging these to D gives:

$$D = \sum_n w_n x_n^2 - \frac{(s_1 + s_2)^2}{1 - (r_1 + r_2)} - \frac{(s_1 + J s_2)^2}{r_1 + J^2 r_2} \quad (3)$$

Similarly to BLS and to paper I, the first term on the right hand side is constant, leaving the rest as the new CB-BLS statistic (times -1):

$$\mathrm{CB-BLS} = \frac{(s_1 + s_2)^2}{1 - (r_1 + r_2)} + \frac{(s_1 + J s_2)^2}{r_1 + J^2 r_2} \quad (4)$$

J, together with the EB inclination and the directional correction, are all attempts to use all available knowledge about the host EB and the expected transit signal shape so reduce the number of free parameters. For this reason CB-BLS uses the simplest possible box-like transit model and concisely avoids even slightly more complicated models that requires an additional free parameter (such as the trapezoidal transit model, limb darkening, etc.). Note however, that the EB model itself can be as complicated as needed - as long as it stays a pre-processing step to CB-BLS it does not add free parameters to the CB-BLS fitting process.

3. blind tests to CB-BLS

CB-BLS was subsequently blind-tested using a detached EB observed during the initial run of CoRoT (CoRoT ID 102806577). The "examiner" (HD) created the test data in four steps: (1) Removal of a constant slope apparent in the data and conversion to relative flux units $(F - F_0)/F_0$, where F_0 is an average of the out-of eclipse flux. (2) Generation of a model light curve (LC) of the EB and removal of this model from the data. (3) On the residuals, suppression of the noise in some band pass and re-addition of random noise in same band pass. This step was intended only to deny the "solver" the ability to use the fact that all test LCs are based on the same system [1]. (4) Adding to the previous data a model LC that consists of the EB model of step (2) together with a simulated circumbinary planet, using the UTM transit simulator [Deeg & Schneider

[1] Otherwise, by subtracting the various test curves from each other one may be able to see were the simulated transits are.

Parameter	Value	Unit
Period	3.6670288245	[d]
Inclination	86.6699982	[deg]
R_1	1.856	$[R_\odot]$
R_2	0.6838	$[R_\odot]$
L_1	14.620	$[L_\odot]$
L_2	0.2500	$[L_\odot]$
RMS of residuals	~ 1.3	[mmag]

Table 1. Main EB parameters that affect the CB planets transit.

2009]. Steps (3) and (4) were repeated six times, simulating different planets in step (4).

The CB-BLS "solver" (AO) then received the six test LCs designated Test0 through Test5, and parameters of the physical model of the system. The solver then independently solved the LC using JKTEBOP [Southworth *et al.* 2004a,b] and applied CB-BLS. For the CB-BLS analysis, only the mass ratio was used out of the full physical model. As written in paper I, if the mass ratio is not known - it can simply be searched-on as a free parameter. Figure 1 depicts the EB itself with the JKTEBOP model (from the Test5 LC), and also the six residuals LCs. Note that the residuals have some structure, meaning, they have red noise – as expected in real data. In Table 1 we list some of the EB's physical model parameters that most affect transit detection. Note that the RMS of the residuals is about 1.3mmag. We comment that each of these CB-BLS analyses take approximately 2min on a 3GHz PC (using the natural parameter resolutions presented in paper I), so processing time is neglible, given the small number of targets relative to constant stars.

The six tests signals where such that Test0 was relatively easy and not blind (it was used primarily to make sure the test procedures are working) - but still the simulated system was a physically-possible system, while Tests 1-5 were completely blind. Fig. 2 shows the resultant CB-BLS periodograms and Table 2 gives the resultant best CB-BLS fits values. All six test LCs were correctly identified, where notably Test5 was correctly identified only when the single-depth CB-BLS of §2.1 was used. As an illustration for the ability to detect even shallow transits significantly, see Fig 3 where the shallowest simulated planet in these tests is shown. Note that this simulated planet caused only three primary transit events, where a primary transit is only ~ 1.4 mmag deep (to be compared with RMS dispersion of 1.3 mmag). This depth corresponds to a planetary radius of $0.73R_J$ in an EB with a primary component with a radius of $1.856R_\odot$. Scaling this depth to $1R_\odot$ (and ignoring the much-fainter secondary component) gives $0.39R_J$ - smaller than the second-smallest known transiting planet HAT-P-11b [Bakos *et al.* 2009]. We conclude that CB-BLS passed the blind tests successfully and is ready for use on real data.

4. Application of CB-BLS to real data

4.1. TrES Lyr1 field

The photometry of the TrES survey Lyr1 field [O'Donovan *et al.* 2006, Dunham *et al.* 2004] is freely available at the NASA NStED website [2], but this photometry is after TrES's detrending, and so can't be used as-is for our purpose. We therefore asked the above authors for the raw photometry of the same data, and we process below only the raw Slueth data - which contributes $\sim 11,000$ data points of the total $\sim 15,000$ of the TrES Lyr1 dataset.

Here we present our first application of CB-BLS to photometry from a real wide-field survey and the following pre-processing scheme is the template for our future applications of CB-BLS. The main difference between the scheme below and the corresponding pre-processing steps of other transit searches is the ability to not only detrend intrinsically-constant stars but also to detrend variable stars by iteratively detrending their residuals. The pre-processing has four main stages:

1. Determination of the systematic effects: This is very similar to what is done routinely on transit surveys. Firstly, outlier data points are removed form all light curves by sigma clipping each light curve around a small-window (5 points) median filter. Next, we wish to determine a few SYSREM effects [Tamuz *et al.* 2005] - but we must make sure that variable stars are not part of the set of stars that is used to determine the effect. To that end we use the Alarm statistic [Tamuz *et al.* 2006] as a general variability statistic (used similarly to the Stetson J statistic [Stetson 1996]) in the following manner (Note that in general Alarm will have a smaller value for less-systematic input): 1) We compute Alarm for all stars 2) we determine the sub-set of constant stars using an Alarm maximal value that corresponds to the bulk of the stars (i.e., many stars that change similarly, so they probably don't have intrinsic variability). See Fig. 4 for an example. 3) The SYSREM effect(s) are computed using only this subset of constant stars (one effect in the above example) and the correction is applied to all the stars, 4) Alarm is re-computed. Since now the bulk Alarm distribution is narrower (e.g., main panel of Fig 4) it allows to better filter true variables - so using a lower Alarm maximal value the set of constant stars is re-determined. Steps 2-4 can be repeated several times till the set of constant stars converges. Note that in each iteration the effects must be always computed from the same raw data and not from the SYSREM-corrected data. This procedure also imporoves the signal-to-noise ratio of the SYSREM effects.

2. Detrending variable stars: The constant stars allowed to determine the systematic effects well - and from now on the effects are assumed known and will not be changed. To correct variable stars for these systematic effects we will have to apply the same correction determined above to the residuals around the smoothed LC of the target variable star by iteratively smoothing the target LC, detrending the residuals, adding back the corrected residuals to the previous smooth and then re-smoothing the LC, till convergence While this procedure is sensitive to the exact smoothing technique, when the smoothing parameters fit well for a given LC the results are quite significant for transit detection (see Fig. 5), and allow to reduce the scatter of the LC around the model to the same level as the scatter of LCs of constant stars of similar brightness.

3. EB solution: Light curves for eclipsing binaries in the Lyr1 field were analyzed by the NDE model. Errant observations were picked out by eye and eliminated before analysis. Accurate dates on minima were determined from the data by using the method of Kwee & van Woerden (1956). The resulting periods and zero epochs are listed in Table 3, along with the fitted orbital parameters. In most

[2] http://nsted.ipac.caltech.edu/

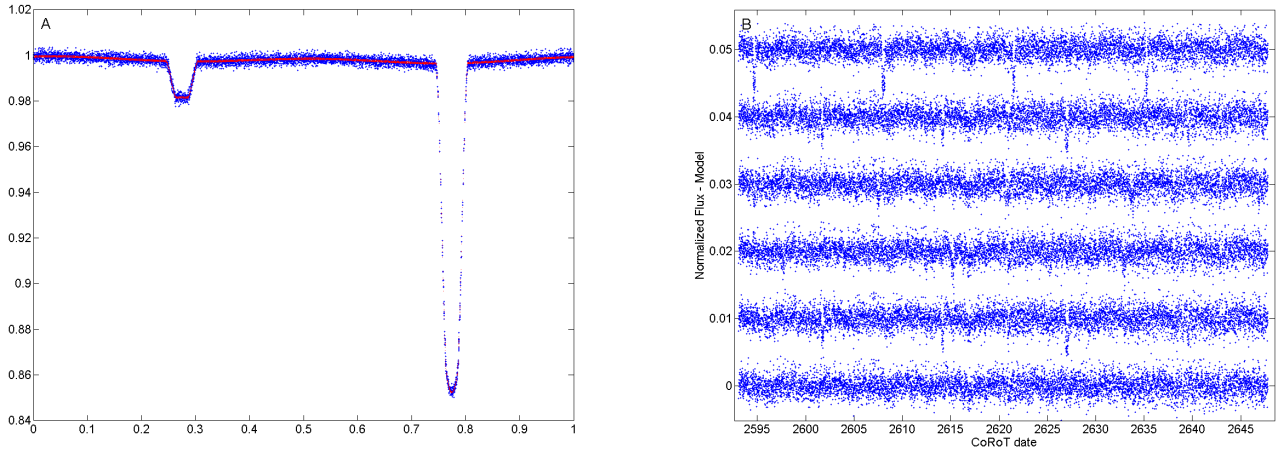

Fig. 1. Panel A: LC of the EB used in the blind tests (dots) and its JKTEBOP model (line). This LC is the Test5 LC which has no planet added to it. Panel B: the residuals of the six test LCs from Test0 (top) to Test5 (bottom). Each successive residuals LC was shifted by 1% to aid visibility.

	Attribute	Detection	period [d]	Epoch [CoRoT date]	depth (pri) [mmag]	Comment
Test0	Examiner		13.54	2594.54	4.756	
	Solver	+++	13.545	2594.525	4.768	Not blind.
Test1	Examiner		12.673	2563.567	2.788	
	Solver	+++	12.667	2595.251	2.494	A bug (since then fixed) caused the detected reference time to be when the planet crossed the baricenter *behind* the EB system, causing a half-integer difference (2.5 periods) from the correct one.
Test2	Examiner		13.08	2594.54	1.907	
	Solver	+++	13.091	2594.513	1.560	
Test3	Examiner		17.748	2597.54	1.952	
	Solver	+++	17.738	2597.571	1.349	
Test4	Examiner		12.673	2563.567	2.788	
	Solver	+++	12.652	2595.295	2.579	See comment to Test1
Test5	Examiner	no planet	-	-	-	
	Solver	no planet	-	-	-	A very weak signal was initially suspected before using the single-depth analysis. That periodogram peak completely disappeared when this feature was added and used.

Table 2. The input values of the simulated CB planets ("Examiner" rows) and their respective solution ("Solver" rows). Note that the simulated planets had their the inclination and position angle varied to some extent - but since these quantities are not derivable from CB-BLS they are not given in this comparison. The simulated depth value is computed by $(R_p/R_s)^2$ - which is only approximated since the simulated transit LCs include limb darkening. The possible detection levels are: "+++" (Strong and secure), "++" (Probable. Noisy), "+" (Weak detection) and "no planet". The reference epoch is the planetary baricenter crossing time. The depth of the secondary transit is omitted since it is simply J times the primary transit.

cases, the fitted light curves were relatively insensitive to the assumed values of the limb-darkening coefficients (x_p and x_s) and to the mass ratio (q), which was guessed based on preliminary values of the light ratio. 5 of the 17 light curves showed significant eccentricity.

4. Generation of final EB LC: Almost identically to the "Detrending variable stars" step - the raw LC is detrended using the solved EB model. Now the model is final so multiple iterations are not needed.

Fig. 6 depicts further examples of EBs from the TrES Lyr1 field, showing that the generation of multiple near-systematics-free EB light curves from wide-field transit surveys using the procedure above is indeed possible. The low level of systematics will help CB-BLS to be less likely to find spurious signals. All in all, about two dozen detached or semi-detached EBs were bright enough (similarly-bright constant stars had ultimate precision of $\sim 2\%$) to be processed as above. Of these 17 EBs were fitted, and for 8 of them planet detection seemed possible (the other EBs exhibit either low inclination angles, evidence of spots or period change), and CB-BLS was applied - but we did not detect any significant signal. We note that currently we don't have robust estimates for detection limits – neither in TrES Lyr1 data or the EBs presented in the next section. We plan to develop procedures for detection limits assessment in the future.

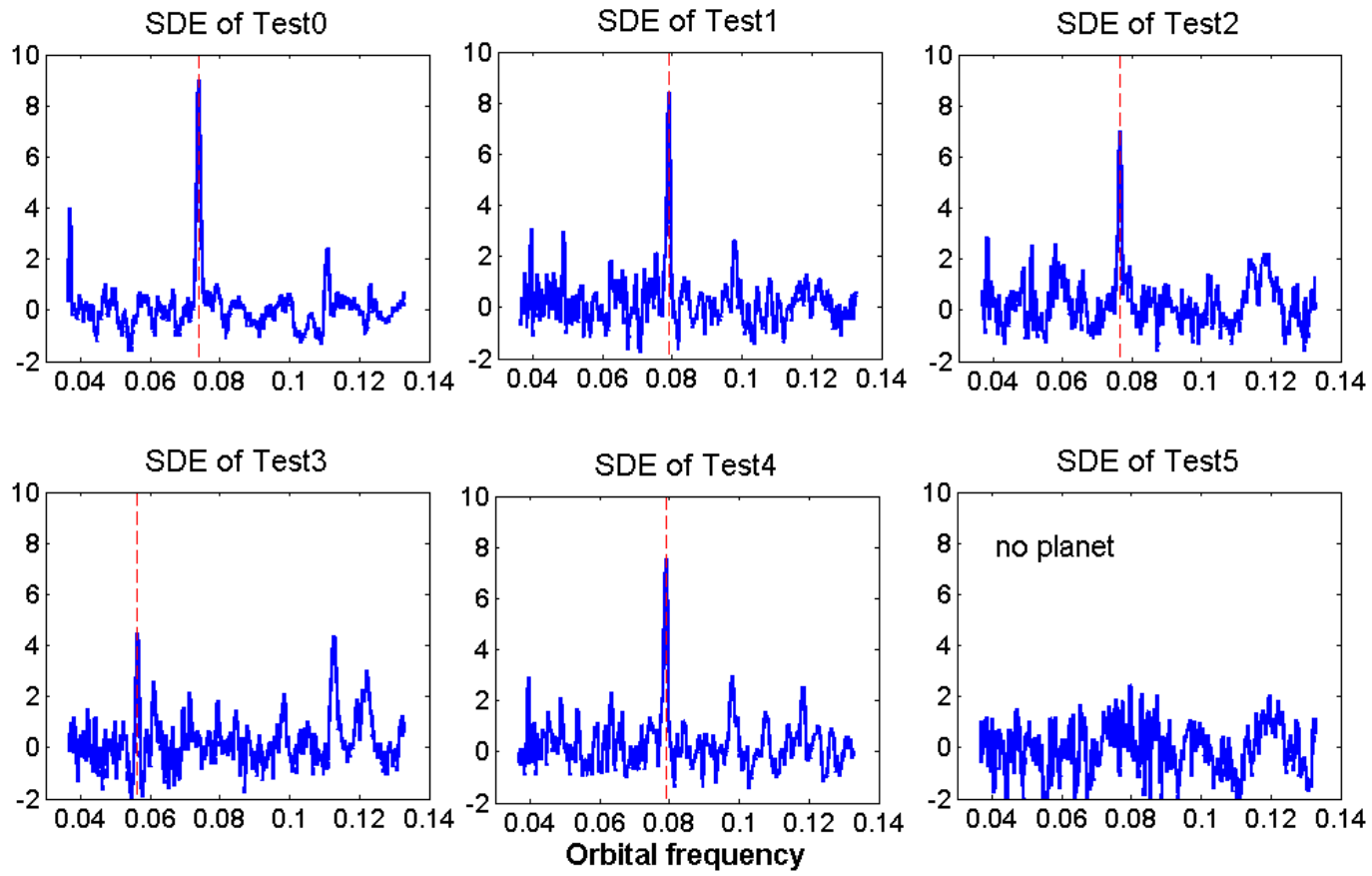

Fig. 2. The straightened periodograms of the blind tests — to be read together with the input and output values specified on Table 2. Note that in Test3 the period is longest, so the first harmonic of the true signal is also visible as the second-highest peak. The highest frequency ($f \sim 0.136d^{-1}$) corresponds to a period just twice that of the binary – near the instability limit. The periodograms are normalized to the their own RMS (as described in Paper I) - and thus effectively equivalent to the SDE metric of BLS [Kovács *et al.* 2002]. Thus, a value of 5 is a 5σ detection of a certain period.

4.2. Other targets

While wide-field transit surveys such as CoRoT will probably be the main source of EBs for future CB-BLS analyses (as demonstrated above), there are currently a number of open literature papers on EBs that have a long enough and accurate enough LCs to possibly allow the detection of transiting planets. These papers focus on the EBs and so have the added benefit having the EBs (usually) fully analyzed - including spectroscopic determination of the mass ratio q (which allows to remove one free parameter, and shorten the CB-BLS run time). Note that for some of these objects the new multi-band CB-BLS feature is required. Also note that while the blind test were conducted on a $\sim 50d$ long LC, these objects were observed over much longer periods – typically several years. This necessitates a correspondingly higher frequency resolution, and consequently – significantly longer CB-BLS run time.

Light curves of WW Cam (Lacy *et al.* 2002) and V1061 Cyg (Torres *et al.* 2006) were taken from the literature and fitted by the NDE model (Etzel 1981, Popper & Etzel 1981) as described above. LC parameters for those stars are listed in the referenced articles. Light curves of V432 Aur [Siviero *et al.* 2004] and BP Vul [Lacy *et al.* 2003] were also taken from the literature and fitted with JKTEBOP – giving LC parameters similar to the ones listed in the referenced articles. In Fig 7 we plot the above LCs together with their best-fitting model and model residuals. We applied CB-BLS to these systems too but did not detect any significant signal.

5. Conclusions

We presented a number of improvements to the CB-BLS algorithm that allow CB-BLS to improve it's sensitivity to shallow transits, correctly model distorted close binary stars, use multi-band photometric data, and more. The resultant implementation of CB-BLS was blind-tested using five test light curves derived from CoRoT data - and were all correctly and strongly identified. We also presented an example of a procedure for the correct detrending of variable stars from wide-field surveys that results in far less systematic input light curves for CB-BLS, and a subsequent first application of CB-BLS to real LCs from both targeted observations and a wide-field survey.

Looking for transiting CB planets requires good understanding of several issues: how to generate good photometry of intrinsically-constant stars (now well understood), how to generate good photometry of intrinsically-variable stars (for e.g., as explained above: iterative detrending of the residuals), high-quality EB modeling, and finally - the

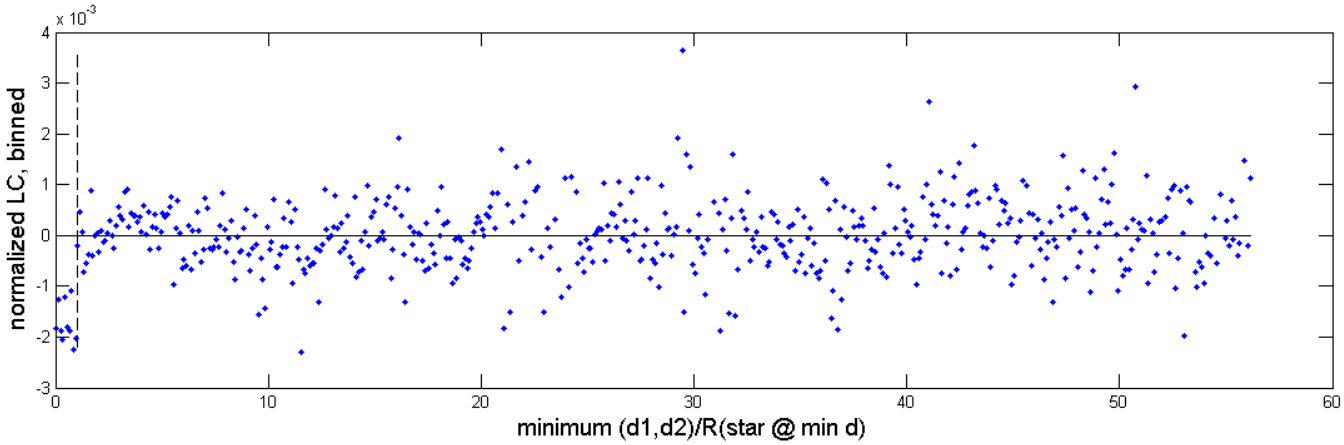

Fig. 3. The Test3 LC residuals folded at the best-fit model. In-transit points are expected when the sky-projected distance between the planet and one of the components is closer than that component's radius. For that reason the data is folded against the minimum distance of the planet from each of the EB components - and that distance is scaled by that star's radius. The result is that all in-transit points are expected below scaled-distance of 1, and all out-of-transit points are expected at scaled-distances grater than 1 (marked with a vertical dashed line). To aid visibility the data is binned to 0.1 units of this scaled-distance. We note that despite the fact that Test3 was the shallowest signal in this blind tests series CB-BLS clearly separates in-transit from out-of-transit points.

Star ID	P [d]	E_0	J_s	r_p	r_s	k	i [deg]	e	ω [deg]	L_3	L_p	L_s	x_p, x_s	$q = \frac{m_s}{m_p}$	σ [mmag]
00442	1.0620113	544.9157	0.577	0.252	0.180	0.714	85.3	0.045	-90.3	0.042	0.775	0.225	0.60	0.863	7.255
00822	2.42759	562.8633	1.03	0.157	0.190	1.21	79.6	0.004	-100.0	0	0.397	0.603	0.60	1.0	7.112
01199	2.696428	555.7985	0.374	0.174	0.083	0.477	90	0.003	-63.0	0.032	0.922	0.078	0.60	0.5	7.804
01679	1.401052	551.8386	0.103	0.292	0.216	0.74	66.5	0	0	0.239	0.947	0.053	0.60	0.67	7.288
02303	1.387197	546.7336	0.049	0.280	0.100	0.358	79.6	0.072	83.8	0	0.994	0.006	0.60	0.368	7.978
03705	4.703549	560.7989	0.793	0.113	0.071	0.63	85.5	0	0	0	0.760	0.240	0.60	0.95	10.146
03708	0.428355	552.7032	0.95	0.377	0.354	0.94	60.9	0	0	0	0.55	0.45	0.60	0.95	14.256
03793	3.472262	545.7911	1.005	0.113	0.100	0.88	87.4	0	0	0.32	0.56	0.44	0.48	0.95	9.754
04063	0.876825	549.8667	0.000	0.398	0.179	0.45	69.7	0	0	0.153	1.000	0.000	0.60	0.29	11.848
04826	1.25042	596.8055	0.302	0.240	0.155	0.65	80.8	0	0	0.20	0.89	0.11	0.60	0.85	10.674
05140	0.903320	554.9364	0.010	0.339	0.203	0.714	84.8	0	0	0.249	0.996	0.004	0.60	0.65	24.129
05911	0.2932419	545.7257	0.66	0.395	0.355	0.90	58.4	0	0	0.625	0.656	0.344	0.60	0.95	14.555
05926	0.7085494	545.8493	0.075	0.455	0.329	0.72	55.4	0	0	0	0.964	0.036	0.60	0.80	14.249
06613	0.7445117	546.8838	0.54	0.55	0.44	0.80	41.8	0	0	0	0.75	0.25	0.60	0.80	16.191
06825	1.801803	551.9185	0.133	0.264	0.242	0.917	88.9	0.205	88.6	0	0.887	0.100	0.40	0.70	18.272
07919	6.5233411	549.9007	0.272	0.260	0.249	0.956	67.3	0	0	0	0.792	0.208	0.60	0.40	18.067
08329	1.322684	593.8688	0.090	0.302	0.186	0.615	89.3	0	0	0	0.967	0.033	0.60	0.60	17.262

Table 3. Results of fitting light curves of bright EBs from the TrES Lyr1 field. Boldfaced star names (NStED ID) indicate that CB-BLS was subsequently applied. The other colomns are: the period P and reference epoch E_0 (in HJD-2453000), the surface brighnes ration J_s, the primary, secondary radii and their ratio r_p, r_s and k, the orbital eccentricity, inclination and argument of periastron passage i, e and ω, the light fraction of third light, primary and secondary components L_3, L_p and L_s, the linear limb-darkening coefficients $x_p = x_s$, the mass ratio $q = \frac{m_s}{m_p}$, the RMS of the data around the model σ, and the number of data points used in the fit N.

actual search for transiting CB planets (e.g., the CB-BLS algorithm). While the above general description will probably remain correct, we are still in the process of learning the details of the process - as exemplified by the still-evolving CB-BLS. Still, we feel that the experience of the single-stars transit surveys allows for an even steeper learning curve (and we remind that single-stars transit surveys had their own learning curve: more than 80% of the known transiting planets today were not known only three years ago).

Looking for CB planets around EBs is advantageous since EBs are already well-aligned to our line of sight. Since theoretical models predict that CB planets will be, at least initially, aligned with their host EB – the chances that CB planets will transit in front of the EB components are relatively high. CB planets in general and transiting CB planets in particular are expected to be particularly beneficial for the general study of extrasolar planets:

- Binaries are a very significant fraction of the total stellar population. Studying planet formation and evolution without including the formation and evolution of planets in binary star systems is surely incomplete.
- Frequency of CB planets depends on assumed planetary formation mechanism, and may allow to distinguish between competing theories.
- After the initial surprises of close-in giant planets and planets in eccentric orbits, detecting CB planets will again substantially diversify the environments that produce and sustain planets.
- Understanding very high precision LCs of transiting planets around single stars is limited by the uncertainty of stellar parameters [e.g., Johnson *et al.* 2008, Gillon *et al.* 2008, and discussion therein]. EBs allow to significantly increase stellar parameters accuracy, so resultant fits to planetary structure models will have smaller error bars.

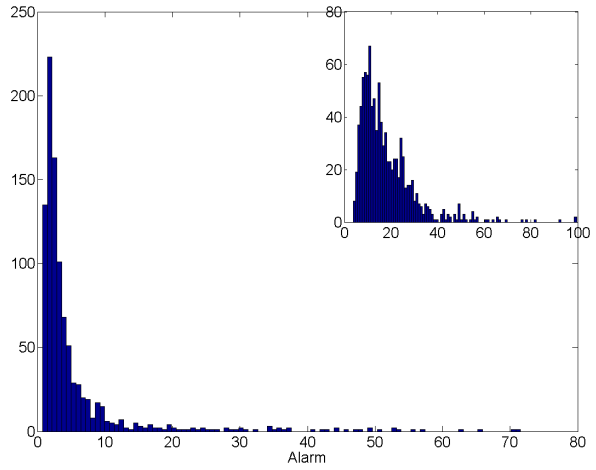

Fig. 4. The Alarm statistic for 1000 objects (all objects in some magnitude range) of the TrES Lyr1 dataset. The insert shows the lower part of the Alarm distribution before the first iteration for variable-stars filtering (see text). After we used only stars with Alarm< 35 to calculate one SYSREM effect - the Alarm distribution of the same objects looked as shown on the main panel.

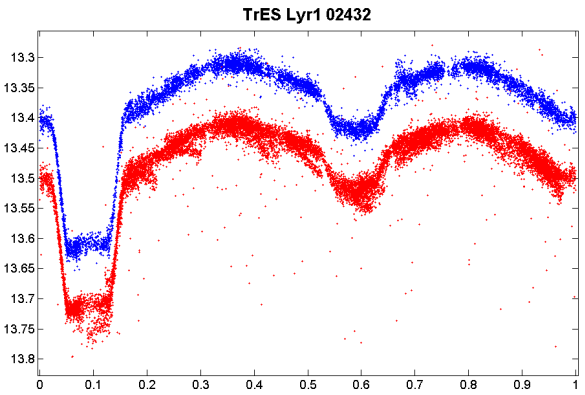

Fig. 5. Two light curves of star 02432 from the TrES Lyr1 field. Bottom, Red LC: the light curve as posted on the public NStED database: it was detrended with no special care for intrinsic variability. Top, Blue LC: the same raw data processed as described in the text - with cleaning procedures applied only to the residuals. Note that transit detection in LCs such as the red LC is nearly impossible.

– Follow up will be interesting for several reasons: I) close-in CB planets can show orbital evolution on short time scales (even 100s of days), II) CB planet systems produce four distinct Rossiter-McLaughlin [e.g., Gaudi & Winn 2007] effects: 1-2, 2-1, p-1 and p-2 (where A-B designates the spectroscopic eclipse of B by A, and 1,2 and p stand for the two binary component and the CB planet, respectively), III) Higher chances of finding resonant systems and/or chaotic systems.

Specifically, using CB-BLS to look for transiting CB planets is especially useful since:

– CB-BLS allows to find shallow transiting CB planets in the residuals of EBs, including sub-noise signals.
– CB-BLS can naturally include Roche geometry - and many EBs require that.

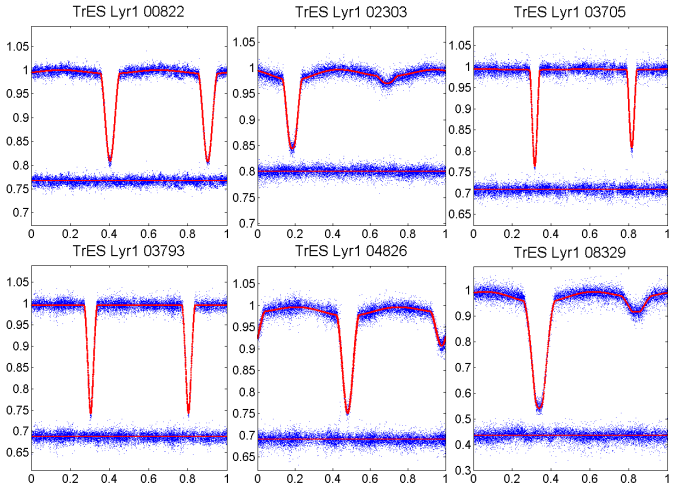

Fig. 6. More examples of the EBs from the TrES Lyr1 field. These EB LCs were generated using the process discussed in the text for the proper detrending of variable stars. This, together with good modeling, resulted in extremely small systematics in the residuals across the $> 11,000$ data points. The object ID at the top of each panel is the NStED designation.

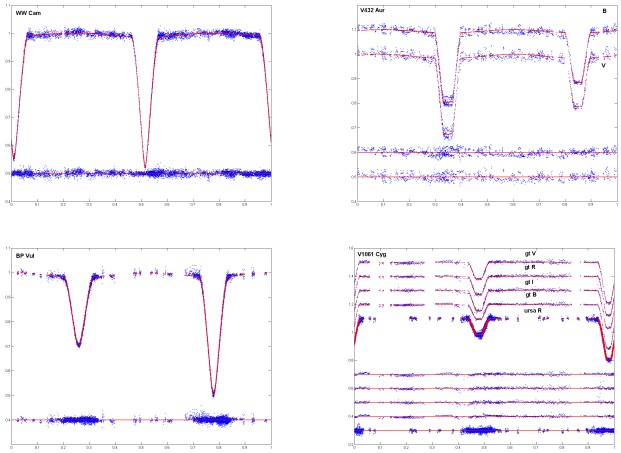

Fig. 7. Some of the open literature EBs to which the CB-BLS analysis was applied. Each EB light curve is phased to it's orbital period with the best-fit model over plotted and the model residuals drawn below.

– CB-BLS can simultaneously fit multi-band data.
– CB-BLS allows to harness existing datasets to the detection of transiting CB planets with no further inputs. Medium (or maybe even low) resolution spectroscopic input can allow to reduce the required CPU time and increase CB-BLS's sensitivity, but is not mandatory.
– CB-BLS source code and documentation are planned to be made freely available. The source code is almost entirely in MATLAB and so easily portable.

6. Acknowledgements

We thank Francis O'Donovan and the rest of the TrES team for making the Lyr1 raw data available to us.

AO is supported by the European Helio- and Asteroseismology Network (HELAS), a major international collaboration funded by the European Commission's

Sixth Framework Programme. HD acknowledges support by grant ESP2007-65480-C02-02 of the Spanish Ministerio de Ciencia e Inovación.

References

Baglin, A., *et al.* 2006, 36th COSPAR Scientific Assembly, 36, 3749
Bakos, G. Á., *et al.* 2009, arXiv:0901.0282
Deeg & Schneider, 2009, to appear in Proc. of 'Transiting Planets', IAU Symposium 253, astro-ph 2008 arXiv0807.3915D.
Dvorak, R. 1986, A&A, 167, 379
Dunham, E. W., Mandushev, G. I., Taylor, B. W., & Oetiker, B. 2004, PASP, 116, 1072
Etzel, P. B. 1981, Photometric and Spectroscopic Binary Systems, 111
Gaudi, B. S., & Winn, J. N. 2007, ApJ, 655, 550
Gillon, M., et al. 2008, arXiv:0812.1998
Holman, M. J., & Wiegert, P. A. 1999, AJ, 117, 621
Johnson, J. A., Winn, J. N., Cabrera, N. E., & Carter, J. A. 2008, arXiv:0812.0029
Kovács, G., Zucker, S., & Mazeh, T. 2002, A&A, 391, 369
Kwee, K. K., & van Woerden, H. 1956, Bull. Astron. Inst. Netherlands, 12, 327
Lacy, C. H. S., Torres, G., Claret, A., & Sabby, J. A. 2002, AJ, 123, 1013
Lacy, C. H. S., Torres, G., Claret, A., & Sabby, J. A. 2003, AJ, 126, 1905
Lee, D.-W., *et al.* 2008b, ApJ, 672, 623
Muterspaugh, M. W., Konacki, M., Lane, B. F., & Pfahl, E. 2007, arXiv:0705.3072
O'Donovan, F. T., et al. 2006, ApJ, 651, L61
Ofir, A. 2008, MNRAS, 387, 1597
Ofir, A. 2009, Box Least Squares (BLS) As An Orbit-Fitting Algorithm - In preperation.
Popper, D. M., & Etzel, P. B. 1981, AJ, 86, 102
Seto, N. 2008, ApJ, 677, L55
Siviero, A., Munari, U., Sordo, R., Dallaporta, S., Marrese, P. M., Zwitter, T., & Milone, E. F. 2004, A&A, 417, 1083
Southworth, J., Maxted, P. F. L., & Smalley, B. 2004a, MNRAS, 351, 1277
Southworth, J., Zucker, S., Maxted, P. F. L., & Smalley, B. 2004b, MNRAS, 355, 986
Stetson, P. B. 1996, PASP, 108, 851
Tamuz, O., Mazeh, T., & Zucker, S. 2005, MNRAS, 356, 1466
Tamuz, O., Mazeh, T., & North, P. 2006, MNRAS, 367, 1521
Tingley, B. 2003, A&A, 408, L5
Torres, G., Lacy, C. H. S., Marschall, L. A., Sheets, H. A., & Mader, J. A. 2006, ApJ, 640, 1018